Geophysical Research Letters

RESEARCH LETTER
10.1029/2020GL087856

Key Points:
- Geophysical imaging suggests that magma reservoirs are often significantly laterally offset from overlying arc volcanoes
- Offset magma reservoirs are more prevalent at small volcanoes, whereas larger volcanoes have more centrally aligned magma storage
- Characterizing edifice topography may help predict subsurface magma storage geometries and guide volcano monitoring networks

Supporting Information:
- Supporting Information S1
- Table S1
- Table S2
- Table S3
- Data Set S1
- Data Set S2

Correspondence to:
A. H. Lerner,
lerner.allan@gmail.com

Citation:
Lerner, A. H., O'Hara, D., Karlstrom, L., Ebmeier, S. K., Anderson, K. R., & Hurwitz, S. (2020). The prevalence and significance of offset magma reservoirs at arc volcanoes. *Geophysical Research Letters*, *47*, e2020GL087856. https://doi.org/10.1029/2020GL087856

Received 6 MAR 2020
Accepted 15 MAY 2020
Accepted article online 15 JUN 2020

The Prevalence and Significance of Offset Magma Reservoirs at Arc Volcanoes

Allan H. Lerner[1], Daniel O'Hara[1], Leif Karlstrom[1], Susanna K. Ebmeier[2], Kyle R. Anderson[3], and Shaul Hurwitz[3]

[1]Department of Earth Sciences, University of Oregon, Eugene, OR, USA, [2]School of Earth and Environment, University of Leeds, Leeds, UK, [3]U.S. Geological Survey, Moffett Field, CA, USA

Abstract Determining the spatial relations between volcanic edifices and their underlying magma storage zones is fundamental for characterizing long-term evolution and short-term unrest. We compile centroid locations of upper crustal magma reservoirs at 56 arc volcanoes inferred from seismic, magnetotelluric, and geodetic studies. We show that magma reservoirs are often horizontally offset from their associated volcanic edifices by multiple kilometers, and the degree of offset broadly scales with reservoir depth. Approximately 20% of inferred magma reservoir centroids occur outside of the overlying volcano's mean radius. Furthermore, reservoir offset is inversely correlated with edifice size. Taking edifice volume as a proxy for long-term magmatic flux, we suggest that high flux or prolonged magmatism leads to more centralized magma storage beneath arc volcanoes by overprinting upper crustal heterogeneities that would otherwise affect magma ascent. Edifice volumes therefore reflect the spatial distribution of underlying magma storage, which could help guide monitoring strategies at volcanoes.

Plain Language Summary Magma reservoirs are commonly assumed to be located directly beneath their associated volcanic edifices. This "central reservoir" paradigm dominates volcano modeling and monitoring. However, the actual spatial relations between volcanoes and underlying magma reservoirs are poorly known. We compile a database of geophysical studies at subduction zone volcanoes where magma reservoirs were detected through subsurface modeling of seismic waves, electrical conductivity, and ground deformation. We then systematically map volcano shapes and compare their center locations with associated magma reservoirs. We find that while the majority of volcanoes are located directly above their source reservoirs, a substantial number of magma reservoirs are laterally offset multiple kilometers from their volcano's centers. Approximately 20% of magma reservoirs are located beyond the "footprints" of their volcanoes. Additionally, magma reservoirs are more laterally offset at small volcanoes, but more centrally aligned at large volcanoes. We propose that increased magma flux at large volcanoes thermally overprints crustal faults and heterogeneities, leading to progressively more centrally focused magmatic systems. Our work suggests that the central reservoir view of volcanic systems should be revised to account for magma focusing as volcanoes grow. Recognizing the global prevalence of laterally offset magmatic systems may better help design volcano monitoring networks.

1. Introduction

Volcano monitoring strategies and models of magma transport in the shallow crust often implicitly assume that magma storage occurs directly under topographic highs of the volcanoes they feed (Moran et al., 2008; Pinel & Jaupart, 2003; Sparks et al., 2012). With an increasing quantity and quality of seismic and magnetotelluric (MT) data, it has been recognized that some magmatic storage zones (hereafter "magma reservoirs") are laterally offset from their associated volcanic edifices (Aizawa et al., 2014; Syracuse et al., 2015; Vargas et al., 2017). Geodetic observations have similarly demonstrated that a substantial proportion of deformation signals occur relatively distant to volcanic edifices (Ebmeier et al., 2018; Lu & Dzurisin, 2014). Lateral offsets are also commonly observed at analog systems such as geysers (Hurwitz & Manga, 2017). However, a systematic compilation and study of offset magma reservoirs at volcanic systems is lacking.

The best available means to assess the locations of magma reservoirs at volcanoes is through geophysical imaging techniques such as seismic and MT tomography, and from inversion of geodetic data. Seismic tomography measures variations in seismic velocities arising from spatially varying lithology, aqueous fluid and

melt fraction, temperature, and crystallographic alignment (Lees, 2007). MT is sensitive to properties controlling electrical conductivity, namely, aqueous fluid fraction, melt fraction, lithology/fluid composition, and fluid connectivity (Chave & Jones, 2012). Geodesy (e.g., InSAR, GPS, leveling) measures displacement of the ground surface due to processes such as magma injection or withdrawal, cooling and crystallization of magma bodies, accumulation of magmatic gases, or pressure changes in shallow hydrothermal systems (Dzurisin & Lu, 2007). These techniques are thus sensitive to different, but contemporaneous, aspects of subsurface magma storage and transport.

Quantifying the global pervasiveness of laterally offset magma reservoirs and their depth distributions relative to volcanic edifice volumes and morphologies (Castruccio et al., 2017; Pinel & Jaupart, 2003), magma compositions and degassing rates (Wallace, 2005), stress states of volcanic arcs (Chaussard & Amelung, 2012; Pinel & Jaupart, 2000) and host rock lithologies (Maccaferri et al., 2011; Taisne & Jaupart, 2009) is critical for identifying the key physical processes that control magma transport in the upper crust. In order to address such questions, we compile a database containing topographic characterizations of volcanic edifices and of geophysically inferred subsurface locations of associated magma reservoirs. We restrict our study to arc volcanoes to limit the potential tectonic variability of hotspot and rift systems. The high threat of many arc volcanoes further motivates the need to better understand these systems.

2. Methods

2.1. Database of Geophysically Inferred Magma Reservoir Locations

We include in our database magma storage locations from studies published between 2000 and 2018 in which authors explicitly locate a reservoir at depths of 2.5 to 15 km below the local mean ground surface, and where the spatial resolution is sufficiently high (kilometer-scale). Shallower reservoirs are excluded to avoid the preponderance of hydrothermal features, which are difficult to distinguish from magmatic features using geophysical methods. These criteria necessarily exclude a number of published studies, but the resulting database still contains 77 inferred magma reservoirs at 56 arc volcanoes. Forty-seven reservoirs are from geodetic inversions and 30 are inferred from seismic and/or MT tomographic models (Figure 1). Owing to the challenges of maintaining consistency between the diverse data sets, we utilize only the magma reservoir centroid positions (latitude, longitude, and depth of the center of tomographic anomalies and modeled deformation sources) rather than attempting to identify the geometry and spatial extent of magma storage. While tomography can identify crustal anomalies with low seismic velocities or high electrical conductivities that may be related to either dynamic or static magma reservoirs, geodetic signals indicate active magmatic processes. Therefore, the centroid of a modeled deformation source is not necessarily the center of a magma reservoir, but rather a region where detectable deformation at depth (commonly attributed to pressure changes) is occurring. Conversely, magmatic tomographic anomalies do not necessarily imply potentially mobile magma, as there is seldom sufficient resolution to identify particular areas of high melt concentration.

2.2. Coupling Geophysical Observations With Surface Topography

Assessing the spatial relation between magma reservoirs and associated volcanic landforms requires a consistent method of characterizing volcanic edifice topography. Most volcanoes are constructed through repeated, localized eruptions and intrusions so that overall volcanic edifice size and shape is a better indicator of the time-averaged locus of volcanic output than the location of an individual vent or volcanic peak. We therefore examine the spatial relations between edifice centroids (the geometrical center of topography, largely determined by low-lying basal area) and magma reservoir centroids. In topographically complicated volcanic settings with flank or nested vents and domes, or where vents have formed along caldera-bounding faults, we consider features of similar age and petrologic character (chemical and isotopic compositions) to be related as an overall volcanic complex. We then treat each complex as a single edifice. Often there is an age progression of structures within volcanic complexes or post-caldera eruptive features, so in viewing volcanic complexes as single edifices we are effectively using a longer timeframe to define the surface expression of a volcanic system. We therefore classify some volcanoes differently than the classification in the Smithsonian Institution database (2013) (Text S2, and Tables S1 and S2 in the supporting information).

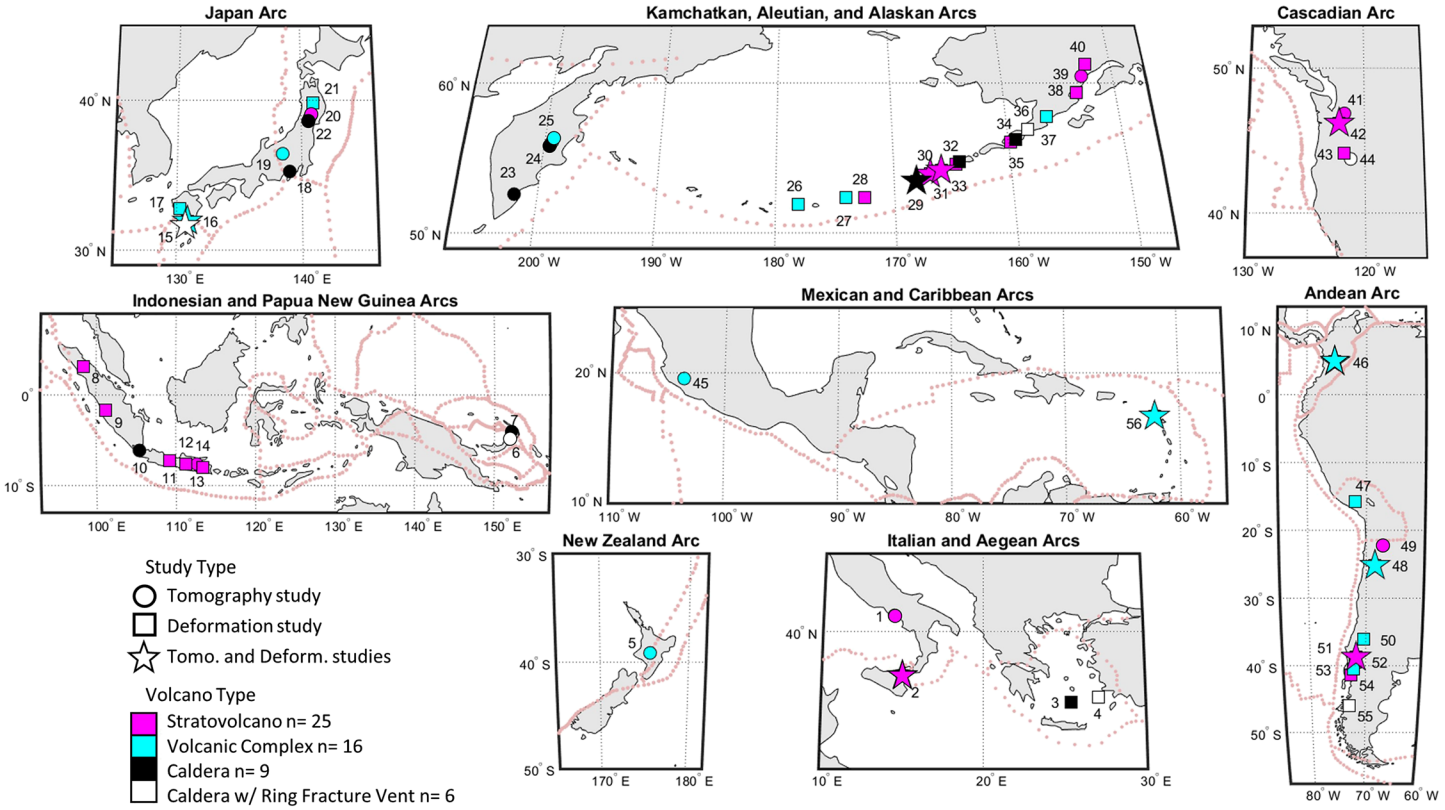

Figure 1. Global distribution of arc volcanoes with geophysically inferred magma reservoirs used in this study. Symbol colors indicate volcanic edifice type and symbol shapes indicate the type of geophysical method. Plate boundaries are mapped in red dashed lines. Volcano numbers relate to information in Tables S1, S2, and Figure S1 in the supporting information.

We characterize the topography of each edifice using a closed contour algorithm (Bohnenstiehl et al., 2012), which fits an adjusted basal contour around a volcano, accounting for background slope and the presence of nearby topographic features. Once the bounds of an edifice are defined, the volume, relief, mean radius, and topographic centroid are calculated (Text S2). This method generally produces a conservative estimate of basal contour and therefore edifice volume. By using this mapping algorithm, coupled with a global 30 m digital elevation model (DEM) (NASA, 2013) and a bathymetry database for subaqueous locations (Amante & Eakins, 2009), we maintain a consistent approach for quantifying edifice geometry.

Based on geophysical data quality (e.g., number of stations, ray path coverage, duration of measurement, goodness of model fits, author-stated confidence) and corroborating data sets (earthquake locations, petrologic geobarometry, observed coeruptive linkages between reservoir locations and edifices), we assign confidence values of low, high, and near-certain (reservoirs with coeruptive links to edifices) to reservoir locations and to their associations with particular volcanoes. Mount St. Helens (WA, USA) provides an example where the location of the syn-eruptive deformation source is consistent with earthquake locations, leading to high confidence in the modeled geodetic source location and connection to the edifice (Figure 2a). In comparison, a reservoir location to the southwest of the volcano that is inferred from seismic tomography does not share such evidence and is assigned a lower confidence factor. However, filtering the data set by this confidence value does not greatly affect the results. A more extensive discussion of methods, data sources, and assessment of confidence is presented in the supporting information Texts S1–S4. Edifice and magma reservoir location parameters can be found in Data Sets S1 (edifice bounds maps) and S2 (Google Earth database).

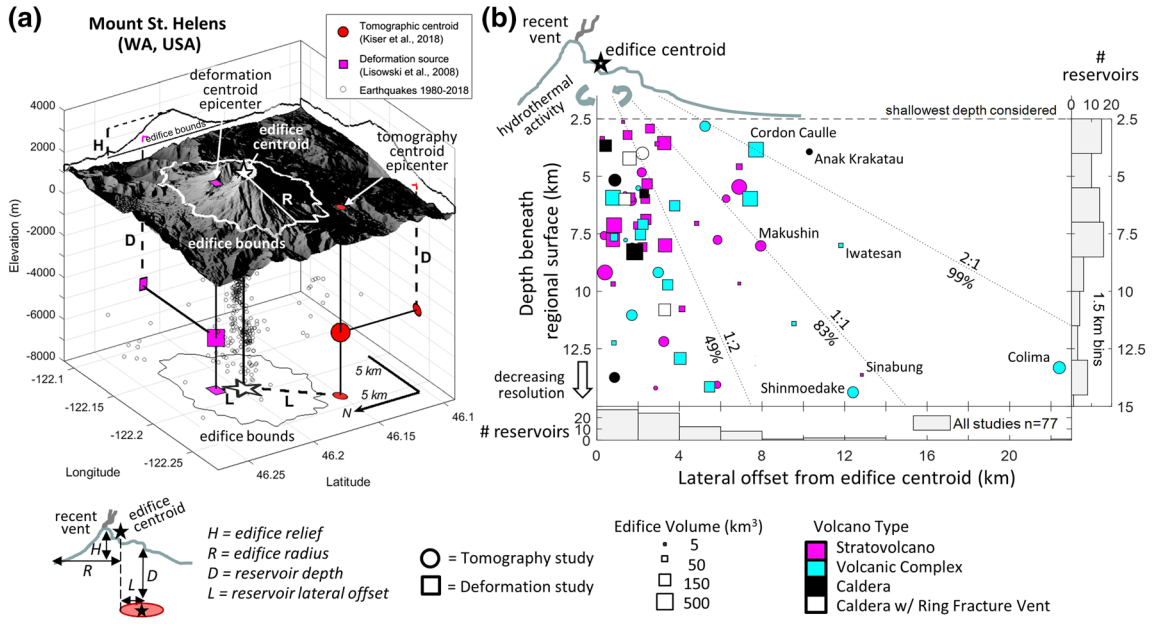

Figure 2. (a) Inferred magma reservoir locations and the volcanic edifice of Mount St. Helens, with the key parameters used in this study labeled. Edifice bounds calculated from surface topography (measured February 2000) are shown in white and projected to the figure base, the star is the calculated edifice centroid, *R* denotes the mean edifice radius from the centroid, and *H* is edifice height. The centroids of magma reservoirs are inferred from seismic tomography (Kiser et al., 2018) and from coeruptive deformation between 2004 and 2006 (Lisowski et al., 2008). *L* is the lateral offset of magma reservoir centroid from edifice centroid, *D* is magma reservoir centroid depth relative to local surface elevation (Texts S1 and S3). Earthquake locations for reviewed events larger than magnitude 1 between 1980 and 2018 are shown for context (n = 10,508; Pacific Northwest Seismic Network [https://pnsn.org/]). (b) Lateral offset and depth distribution of magma reservoir centroids relative to their associated volcanic edifices for the global data set. The percentages of magma reservoirs occurring within different lateral offset to depth ratios are shown. Symbols are classified by volcano type (color) and whether the magma reservoirs were inferred tomographically (circles) or geodetically (squares). Symbol size scales with edifice volume. Thirteen magma reservoirs at volcanoes with unquantified edifice volumes are included in the vertical and horizontal histograms but are not shown in the main plot.

3. Results and Discussion

3.1. Distribution of Magma Reservoirs Beneath Arc Volcanoes

We define reservoir "lateral offset" as the horizontal distance from a magma reservoir centroid to an associated volcanic edifice centroid (Figure 2a). As the spatial scale of volcanic edifices varies widely (mean radii range from 2 to 16 km in our database), it is also useful to define reservoir "scaled offset" as the magma reservoir lateral offset relative to the mean edifice radius (Figure 3). Considering these metrics, we find the following relations:

3.1.1. Central and Offset Reservoirs

Although the majority of magma reservoir centroids underlie their respective edifices, more than one third (34%) are offset by ≥4 km from their edifice centroids (Figure 2b, Table S3, and Figure S5). Eighteen percent of the reservoir centroids are outside the "footprint" of their associated edifice, defined as >1 mean radius distance from the edifice centroid (Figure 3). Basalt-dominated systems have somewhat more centrally aligned reservoirs compared to more silicic volcanoes (Figures S9 and S15). The degree of reservoir offset has no apparent relation to arc stress regime, subduction convergence direction, or SO_2 degassing rate (Figures S2, S3, S12, and S13). Overall, magma reservoirs are slightly more aligned with edifice centroid locations than with recent eruptive vents or summit locations (Figures S8 and S9).

3.1.2. Reservoir Depths

Magma reservoirs occur throughout the entire 2.5–15 km depth range considered in the data set (Figure 2b). However, the sensitivity of geophysical techniques generally decreases with depth, so it is probable that deeper magma reservoirs are underrecorded. Noting this caveat, we find that magma reservoirs in the full data set have a mean depth of 7.4 ± 3.4 km (6.9 km median). Reservoirs with observed coeruptive links have a similarly large depth range of 7.1 ± 3.4 km (Table S3). Assuming an upper crustal density of 2.75 g/cm^3, the 7.4 ± 3.4 km mean depth of the full data set translates to storage pressures of 2.0 ± 0.9 kbar. This

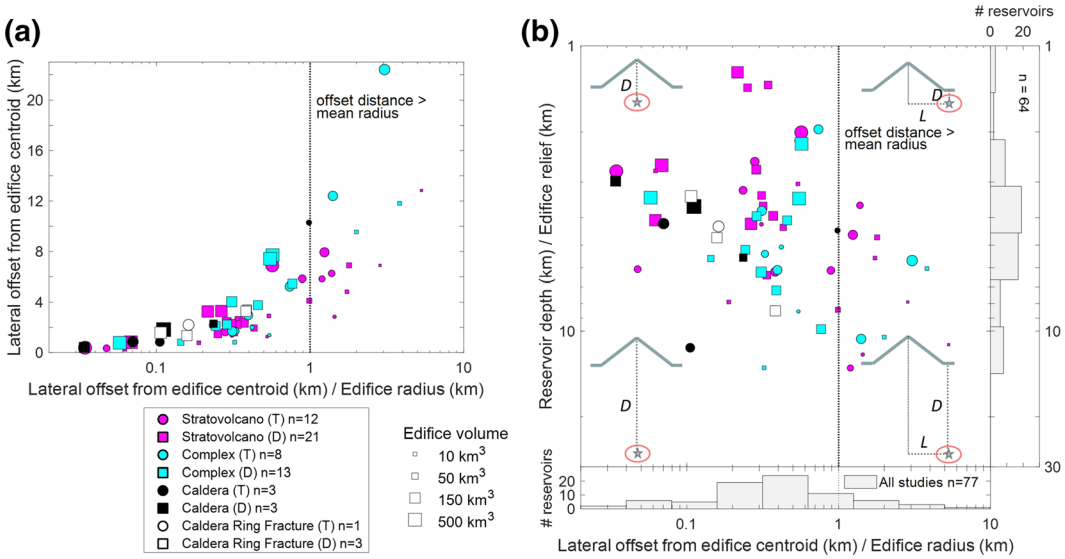

Figure 3. (a) Magma reservoir absolute offsets compared to scaled offsets. Edifice centroids with scaled offsets >1 fall outside the "footprint" of the edifice. Most magma reservoirs with substantial absolute and scaled offsets occur under smaller volcanoes. (b) Nondimensional view of reservoir offset relative to depth, showing that when scaled to edifice height and radius, magma reservoirs at smaller edifices are relatively deeper and more offset, as schematically depicted (*D* is depth; *L* is lateral offset). The database is limited to reservoirs between 2.5 and 15 km depth, which may explain the general lack of reservoirs in the lower left quadrant. Symbol shape, color, and size are as defined in Figure 2. *(T)* and *(D)* indicate tomography and deformation studies, respectively. Thirteen magma reservoirs at volcanoes with unquantified edifice volumes are included in the horizontal histogram but are not shown in the other plots.

pressure range encompasses most of the upper crust and is nearly double the range of magma storage pressures of 2.0 ± 0.5 kbar proposed by Huber et al. (2019). Within the granularity of our compilation, volcanoes with dacitic and rhyolitic compositions tend to have shallower reservoirs than more mafic systems (Figures S9 and S16). We find no apparent correlation between reservoir depth and the regional stress regime, in contrast to previous interpretations (Chaussard & Amelung, 2012) (Figure S2).

Larger lateral offsets are more commonly observed when magma reservoirs are deeper (Figure 2b): 49% ($n = 38$) of reservoirs occur within an area beneath edifices defined by the 1:2 slope of offset to reservoir depth, whereas 83% ($n = 64$) occur within a 1:1 contour and 99% ($n = 77$) occur within a 2:1 contour. This implies a distributed catchment area for rising magma beneath edifices (Ebmeier et al., 2018; Karlstrom et al., 2009). Arc volcanoes with calderas are more commonly associated with shallower, central magma reservoirs (Figures 2b, S15, and S16), consistent with models of collapse calderas involving relatively shallow evacuated magma reservoirs (Acocella, 2007; Lipman, 1997). Geophysical observations of many calderas with ring fracture vents in the database suggest the presence of multiple reservoirs, typically with a shallow reservoir close to the post-caldera ring fracture vent and a deeper reservoir more centrally located under the caldera (Tables S1 and S2).

3.2. Relations Between Magma Reservoir Locations and Edifice Volumes

We find that magma reservoirs beneath smaller edifices are generally more offset, both in absolute and scaled distances (Figures 3a and 3b). Edifice volumes form a continuum over >3 orders of magnitude (Grosse et al., 2014; Karlstrom et al., 2018), and range from 6 to 730 km^3 in our database, with a relatively continuous distribution (Figures S4 and S14). At volcanoes with edifice volumes ≤43 km^3 (for reference, the volume of Mount St. Helens (Figure 2a)), 50% of reservoir centroids are located >4 km from the edifice centroid ($n = 10$ of 20), whereas only 23% of reservoir centroids at larger volcanoes are offset >4 km ($n = 10$ of 44). Similarly, 45% of reservoirs at volcanoes with edifice volumes ≤43 km^3 are laterally offset beyond their edifice radii (scaled offset >1), but only 7% of reservoirs at larger volcanoes are offset to this degree (Figures 3a and S5). Most volcanoes with reservoir scaled offsets >1 are small volume andesitic stratovolcanoes or volcanic complexes (Figure S4). There are no notable differences in reservoir depths beneath small and large volcanoes within the upper 15 km of crust (Figures 2b and S16), in contrast to some model predictions (Castruccio et al., 2017). Lastly, we note that magma reservoir locations

inferred from tomographic models and from inversions of geodetic data conducted at the same volcano often differ substantially, diverging up to 4–10 km horizontally and 2–8 km vertically (Text S1 and Figure S7). Such differences are likely a result of surface displacements being generated by pressure changes in only part of a larger reservoir system, as well as differences in the sensitivities of the geophysical techniques (Dzurisin & Lu, 2007; Ebmeier et al., 2018; Lees, 2007).

3.3. Controls on Magma Reservoir Geometry

The established relation between edifice volumes and the degree to which magma storage is located beneath arc volcanoes has significant implications for modeling magma transport and for volcano monitoring. For example, more laterally offset reservoirs at smaller volcanoes suggests that volcano size encodes some geometrical aspects of the subsurface transport network. Smaller volcanoes are indicative of low-flux or thermally immature systems with shorter histories of volcanic effusion. We infer that low-flux and/or young systems have less centralized magma storage and transport networks than systems with higher magma flux or longer durations of magmatic activity. Further, we propose that this observed relationship is related to a loss of crustal heterogeneity due to the degree of heating, changes to deviatoric stress, and lithologic replacement of host rock by magma intrusions (Figure 4). Such homogenization is a function of the magnitude and the duration of mass and heat input into the shallow crust (Annen & Sparks, 2002; Karlstrom et al., 2017). In systems with more limited magma flux into and through the shallow crust, preexisting structural and stress heterogeneities may more significantly influence ascending magma. For example, horizontal or inclined faults (Galland et al., 2007) and lithologic contacts (Magee et al., 2016) facilitate lateral magma transport and the development of laterally offset reservoirs, as do preexisting background stresses (Maccaferri et al., 2011). Indeed, a number of volcanoes with laterally offset reservoirs occur near major crustal faults (Jay et al., 2014; Lundgren et al., 2015; White & McCausland, 2016).

In contrast, systems with a high magma flux and/or long histories of volcanism alter the shallow crust through cycles of repeated heating, stress changes and intrusion. Deviatoric stresses associated with transient magma storage and volcanic edifice loads may focus dike propagation (Maccaferri et al., 2011; Pinel & Jaupart, 2004; Roman & Jaupart, 2014) and concentrate heat at shallow depths beneath volcanoes. This transport eventually replaces the crustal column and establishes the lateral region of thermomechanically focused magma ascent beneath volcanoes. As crustal impediments to vertical dike ascent are overprinted, eruption locations may become more aligned with the underlying reservoir, causing the volcanic edifice position to progressively migrate. The load of this evolving edifice contributes to further focusing dike ascent, and the magma reservoir may similarly migrate in adjustment to the changing thermal state of the shallow crust (Figure 4b). We propose that, over time, these self-reinforcing mechanisms at high-flux magmatic systems result in larger volcanic edifices being centered above their magma storage zones.

The nature of mechanical coupling between edifice loads and magma reservoirs depends on the wavelength of edifice topography compared to reservoir depth. In the database, all reservoir centroid depths are within an order of magnitude of their edifice diameters (Figure S6), implying that the elastic stress and deformation fields associated with the edifice load and reservoir should interact (McTigue & Segall, 1988). Scaling reservoir depths by edifice relief, which sets the magnitude of the surface load, we find that reservoirs are generally deeper relative to the overlying edifice as they become more offset (Figure 3b), consistent with a distributary region of magma supply.

3.4. Relevance for Monitoring Active Volcanoes

With a simple determination of edifice shape from a DEM (radius, relief, centroid), we can estimate the lateral extent in which underlying shallow crustal reservoirs are likely to occur (Figures 2b and 3). This estimation can be further refined by quantifying edifice size, since large volcanoes are more likely to have centralized magmatic reservoirs compared with smaller volcanoes.

For example, Mount Hood in Oregon (USA) is a high-threat andesitic stratovolcano (Ewert et al., 2018), but there are no constraints on the location of its magma reservoir(s). Based on the calculated edifice topography of Mount Hood (2,350 m relief, 6.5 km mean radius, 89 km^3 volume) and assuming a reservoir depth of 6 ± 2 km from geobarometry (Cooper & Kent, 2014), the relation presented in Figure 3b (with 80% prediction intervals; Figure S17) suggests that the magma reservoir centroid is likely to be within 6 km of the edifice centroid (where the edifice centroid is ~1 km SE of the summit (Data Sets S1 and S2)). In contrast, Mount

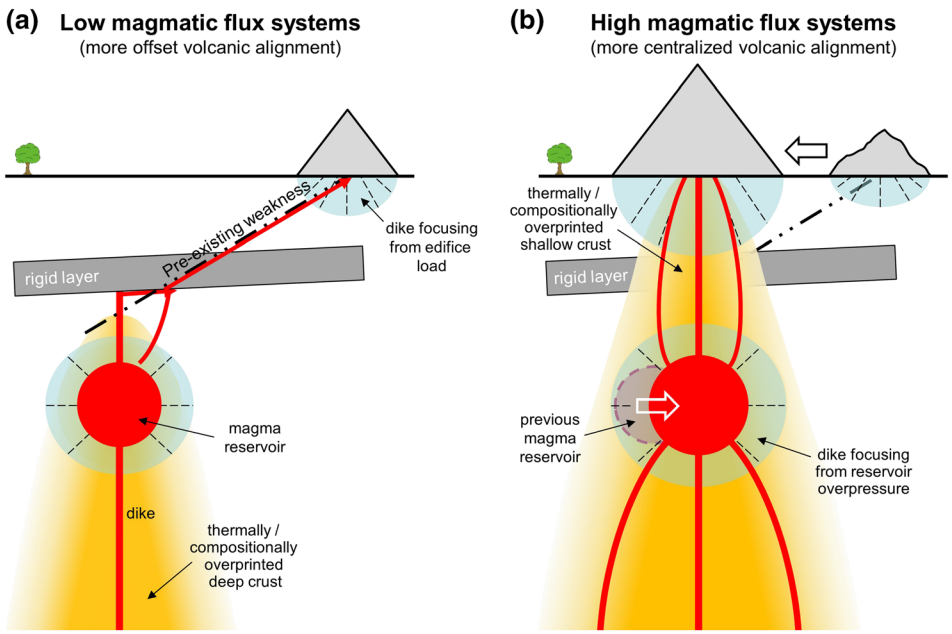

Figure 4. Schematic representation of a magma reservoir and transport system at low- and high-flux volcanoes. (a) Small volcanoes may be a consequence of low magnitude or short-lived magmatic flux. In low-flux systems, much of the upper crust retains heterogeneities that may cause increased lateral transport of magma along zones of weakness (e.g., rheologically competent strata blocking or diverting dike propagation to along faults or between lithologic contacts). (b) Large volcanoes reflect more long-lived or high-flux magmatic systems, which can overprint crustal heterogeneities leading to more focused vertical dike ascent. Magma reservoir locations may similarly migrate in response to changing edifice locations (white arrows). These self-reinforcing processes can contribute to progressively more aligned volcanic systems through time.

Bachelor (also in Oregon) is a smaller Holocene basaltic stratovolcano (900 m relief, 2.7 km mean radius, 8 km^3 volume) and may host a magma reservoir offset by up to 9 km from its edifice centroid, assuming a reservoir depth equal to the mean depth for basaltic reservoirs in the data set (6.8 $\pm$ 2.4 km).

The relatively common occurrence of offset reservoirs warrants reassessing the design of monitoring networks at arc volcanoes. Focusing monitoring instruments exclusively on an edifice or on a particular eruptive vent might miss early signs of unrest at offset systems (Ebmeier et al., 2018). Ground-based monitoring networks or satellite survey footprints may thus be planned more strategically based on simple characterization of the edifice topography. Barring a priori knowledge of subsurface magma reservoir geometry, monitoring coverage should be expanded at smaller volcanoes given their increased likelihood of being associated with more offset reservoirs. Additionally, as edifice centroids tend to be more aligned with magma reservoirs than recent eruptive vents or summits, focusing monitoring networks around edifice centroids rather than vent or summit locations might enable better detections of unrest.

Finally, laterally offset magma reservoirs require horizontal or inclined pathways of magma ascent to the surface (Aizawa et al., 2014; Aoki et al., 2013; Wicks et al., 2011). Nonvertical transport pathways are not commonly included in models for dike propagation and could alter interpretations of geophysical monitoring signals (Rivalta et al., 2015; White & McCausland, 2016). Inclined dikes may also facilitate fluid phase separation during transport, with implications for magmatic degassing and modeling of conduit dynamics (Massol et al., 2001; Vandemeulebrouck et al., 2014).

4. Conclusions and Future Research

By combining geophysical and volcanic landform topography data sets we have identified new constraints on the subsurface geometry of shallow arc magma transport. In particular, we find that magma reservoirs are commonly offset from the presumed volcanic edifices they source. We observe that laterally offset magma reservoirs are more prevalent at small volume volcanoes than at large volcanoes and consequently propose that the magnitude and duration of magmatic flux influences the degree of vertical alignment between edifices and reservoirs. This hypothesis implies that shallow magma storage zones and volcanic

edifice positions evolve through time to become large systems with well-developed, centrally aligned magma transport. The characterization of volcanic edifice topography thus informs the subsurface geometry of shallow magma storage, which may help guide the spatial design of volcano monitoring networks.

An improved ability to consistently constrain geometries and volumes of magma reservoirs would significantly build upon our analysis. For example, dikes may initiate from the edges of magmatic storage zones so that transport pathways could be located away from the centroids of large reservoirs. Further efforts to combine geophysical and topographic data sets from other arc and nonarc volcanoes, along with studies that constrain volcanic histories, will be required to validate the hypothesis that edifice growth corresponds to the centralization of magma transport. Integrating edifice topography and magma reservoir locations with local tectonic features, substrate lithologies, durations of magmatism, and edifice growth and collapse histories has great potential for improving our understanding of the coevolution of volcanic edifices and underlying magma storage and transport systems.

We hope the compilation and observations presented here motivate further efforts to (a) expand and refine similar geophysical and topographic data sets at volcanoes worldwide, (b) assess thermomechanical interactions between edifices and reservoirs to understand the origin and impacts of offset reservoirs, (*c*) more routinely publish the centroids of major tomographic anomalies and pressure sources (with uncertainties) in future geophysical studies, and (d) reconsider what criteria are used to define volcano locations (e.g., vents or edifice centroids), edifice boundaries, and volcano structures.

Data Availability Statement

Data sets for this research are available at this site (https://doi.org/10.7910/DVN/LHD1HY).

Acknowledgments

A. H. L. and D. O. acknowledge support from the National Science Foundation Graduate Research Fellowship Program under Grant 1309047. L. K. acknowledges funding through NSF CAREER 1848554. S. K. E. is supported by a UKRI NERC Independent Research Fellowship and also acknowledges a European Space Agency Living Planet Fellowship and the NERC-BGS Centre for Observation and Modeling of Earthquakes, Volcanoes, and Tectonics (COMET). K. R. A. and S. H. were funded by the U.S. Geological Survey's Volcano Hazards Program. A. L. thanks the University of Oregon geophysics community for many fruitful discussions on tomography methodology and interpretation. We thank Mike Poland and two anonymous reviewers for constructive comments that significantly improved this manuscript, and thank Chris Huber for editorial handling. Any use of trade, firm, or product names is for descriptive purposes and does not imply endorsement by the U.S. Government. We declare no competing interests.

References

Acocella, V. (2007). Understanding caldera structure and development: An overview of analogue models compared to natural calderas. *Earth-Science Reviews*, *85*(3–4), 125–160.

Aizawa, K., Koyama, T., Hase, H., Uyeshima, M., Kanda, W., Utsugi, M., et al. (2014). Three-dimensional resistivity structure and magma plumbing system of the Kirishima volcanoes as inferred from broadband magnetotelluric data. *Journal of Geophysical Research: Solid Earth*, *119*, 198–215. https://doi.org/10.1002/2013JB010682

Amante, C., & Eakins, B. W. (2009). ETOPO1 1 arc-minute global relief model procedures, data sources and analysis: NOAA Technical Memorandum NESDIS NGDC-24. *National Geophysical Data Center, NOAA*, *10*(V5C8276M).

Annen, C., & Sparks, R. S. J. (2002). Effects of repetitive emplacement of basaltic intrusions on thermal evolution and melt generation in the crust. *Earth and Planetary Science Letters*, *203*(3), 937–955. https://doi.org/10.1016/S0012-821X(02)00929-9

Aoki, Y., Takeo, M., Ohminato, T., Nagaoka, Y., & Nishida, K. (2013). Structural controls on magma pathways beneath Asama volcano, Japan. *Geological Society, London, Special Publications*, *380*, 67–84.

Bohnenstiehl, D. R., Howell, J. K., White, S. M., & Hey, R. N. (2012). A modified basal outlining algorithm for identifying topographic highs from gridded elevation data, part 1: Motivation and methods. *Computers & Geosciences*, *49*, 308–314.

Castruccio, A., Diez, M., & Gho, R. (2017). The influence of plumbing system structure on volcano dimensions and topography. *Journal of Geophysical Research: Solid Earth*, *122*, 8839–8859. https://doi.org/10.1002/2017JB014855

Chaussard, E., & Amelung, F. (2012). Precursory inflation of shallow magma reservoirs at West Sunda volcanoes detected by InSAR. *Geophysical Research Letters*, *39*, L21311. https://doi.org/10.1029/2012GL053817

Chave, A. D., & Jones, A. G. (2012). *The magnetotelluric method: Theory and practice* (pp. 1–584). New York: Cambridge University Press.

Cooper, K. M., & Kent, A. J. (2014). Rapid remobilization of magmatic crystals kept in cold storage. *Nature*, *506*(7489), 480–483. https://doi.org/10.1038/nature12991

Dzurisin, D., & Lu, Z. (2007). Interferometric synthetic-aperture radar (InSAR). In D. Dzurisin (Ed.), *Volcano deformation: Geodetic monitoring techniques* (pp. 153–194). Berlin, Heidelberg: Springer Praxis.

Ebmeier, S. K., Andrews, B. J., Araya, M. C., Arnold, D. W. D., Biggs, J., Cooper, C., et al. (2018). Synthesis of global satellite observations of magmatic and volcanic deformation: Implications for volcano monitoring and the lateral extent of magmatic domains. *Journal of Applied Volcanology*, *7*(1), 2. https://doi.org/10.1186/s13617-018-0071-3

Ewert, J. W., Diefenbach, A. K., & Ramsey, D. W. (2018). *2018 update to the U.S. Geological Survey national volcanic threat assessment*. U.S. Geological Survey Scientific Investigations Report 2018–5140, 40 p., https://doi.org/10.3133/sir20185140

Galland, O., Cobbold, P. R., de Bremond d'Ars, J., & Hallot, E. (2007). Rise and emplacement of magma during horizontal shortening of the brittle crust: Insights from experimental modeling. *Journal of Geophysical Research*, *112*, B06402. https://doi.org/10.1029/2006JB004604

Grosse, P., Euillades, P. A., Euillades, L. D., & de Vries, B. van W. (2014). A global database of composite volcano morphometry. *Bulletin of Volcanology*, *76*(1), 1–16.

Huber, C., Townsend, M., Degruyter, W., & Bachmann, O. (2019). Optimal depth of subvolcanic magma chamber growth controlled by volatiles and crust rheology. *Nature Geoscience*, *12*(9), 762–768.

Hurwitz, S., & Manga, M. (2017). The fascinating and complex dynamics of geyser eruptions. *Annual Review of Earth and Planetary Sciences*, *45*, 31–59.

Smithsonian Institution. (2013). Volcanoes of the world, v. 4.3.4 [data set]. Global volcanism program.

Jay, J., Costa, F., Pritchard, M., Lara, L., Singer, B., & Herrin, J. (2014). Locating magma reservoirs using InSAR and petrology before and during the 2011–2012 Cordón Caulle silicic eruption. *Earth and Planetary Science Letters*, *395*, 254–266.

Karlstrom, L., Dufek, J., & Manga, M. (2009). Organization of volcanic plumbing through magmatic lensing by magma chambers and volcanic loads. *Journal of Geophysical Research*, *114*, B10204 https://doi.org/10.1029/2009JB006339
Karlstrom, L., Paterson, S. R., & Jellinek, A. M. (2017). A reverse energy cascade for crustal magma transport. *Nature Geoscience*, *10*(8), 604.
Karlstrom, L., Richardson, P. W., O'Hara, D., & Ebmeier, S. K. (2018). Magmatic landscape construction. *Journal of Geophysical Research: Earth Surface*, *123*, 1710–1730. https://doi.org/10.1029/2017JF004369
Kiser, E., Levander, A., Zelt, C., Schmandt, B., & Hansen, S. (2018). Focusing of melt near the top of the Mount St. Helens (USA) magma reservoir and its relationship to major volcanic eruptions. *Geology*, *46*(9), 775–778.
Lees, J. M. (2007). Seismic tomography of magmatic systems. *Journal of Volcanology and Geothermal Research*, *167*(1–4), 37–56. https://doi.org/10.1016/j.jvolgeores.2007.06.008
Lipman, P. W. (1997). Subsidence of ash-flow calderas: Relation to caldera size and magma-chamber geometry. *Bulletin of Volcanology*, *59*(3), 198–218.
Lisowski, M., Dzurisin, D., Denlinger, R. P., & Iwatsubo, E. Y. (2008). Analysis of GPS–measured deformation associated with the 2004–2006 dome-building eruption of Mount St. Helens, Washington. In D. R. Sherrod, W. E. Scott, & P. H. Stauffer (Eds.), *A volcano rekindled: The renewed eruption of Mount St. Helens, 2004–2006* (pp. 281–300). US Geological Survey.
Lu, Z., & Dzurisin, D. (2014). In *InSAR imaging of Aleutian volcanoes* (pp. 1–390). Berlin, Heidelberg: Springer Praxis.
Lundgren, P., Samsonov, S. V., López Velez, C. M., & Ordoñez, M. (2015). Deep source model for Nevado del Ruiz volcano, Colombia, constrained by interferometric synthetic aperture radar observations. *Geophysical Research Letters*, *42*, 4816–4823. https://doi.org/10.1002/2015GL063858
Maccaferri, F., Bonafede, M., & Rivalta, E. (2011). A quantitative study of the mechanisms governing dike propagation, dike arrest and sill formation. *Journal of Volcanology and Geothermal Research*, *208*(1–2), 39–50.
Magee, C., Muirhead, J. D., Karvelas, A., Holford, S. P., Jackson, C. A., Bastow, I. D., et al. (2016). Lateral magma flow in mafic sill complexes. *Geosphere*, *12*(3), 809–841.
Massol, H., Jaupart, C., & Pepper, D. W. (2001). Ascent and decompression of viscous vesicular magma in a volcanic conduit. *Journal of Geophysical Research*, *106*, 16,223–16,240. https://doi.org/10.1029/2001JB000385
McTigue, D. F., & Segall, P. (1988). Displacements and tilts from dip-slip faults and magma chambers beneath irregular surface topography. *Geophysical Research Letters*, *15*, 601–604.
Moran, S. C., Freymueller, J. T., LaHusen, R. G., McGee, K. A., Poland, M. P., Power, J. A., et al. (2008). Instrumentation recommendations for volcano monitoring at US volcanoes under the National Volcano Early Warning System. *U.S. Geological Survey Scientific Investigations Report 5114*.
NASA JPL. (2013). NASA shuttle radar topography mission Global 1 arc second [data set]. NASA LP DAAC. Retrieved from https://doi.org/10.5067/MEaSUREs/SRTM/SRTMGL1.003
Pinel, V., & Jaupart, C. (2000). The effect of edifice load on magma ascent beneath a volcano. *Philosophical transactions of the Royal Society of London. Series A: Mathematical. Physical and Engineering Sciences*, *358*(1770), 1515–1532.
Pinel, V., & Jaupart, C. (2003). Magma chamber behavior beneath a volcanic edifice. *Journal of Geophysical Research*, *108*(B2), 2072. https://doi.org/10.1029/2002JB001751
Pinel, V., & Jaupart, C. (2004). Magma storage and horizontal dyke injection beneath a volcanic edifice. *Earth and Planetary Science Letters*, *221*(1–4), 245–262.
Rivalta, E., Taisne, B., Bunger, A. P., & Katz, R. F. (2015). A review of mechanical models of dike propagation: Schools of thought, results and future directions. *Tectonophysics*, *638*, 1–42.
Roman, A., & Jaupart, C. (2014). The impact of a volcanic edifice on intrusive and eruptive activity. *Earth and Planetary Science Letters*, *408*, 1–8.
Sparks, R. S. J., Biggs, J., & Neuberg, J. W. (2012). Monitoring volcanoes. *Science*, *335*(6074), 1310–1311. https://doi.org/10.1126/science.1219485
Syracuse, E. M., Maceira, M., Zhang, H., & Thurber, C. H. (2015). Seismicity and structure of Akutan and Makushin volcanoes, Alaska, using joint body and surface wave tomography. *Journal of Geophysical Research: Solid Earth*, *120*, 1036–1052. https://doi.org/10.1002/2014JB011616
Taisne, B., & Jaupart, C. (2009). Dike propagation through layered rocks. *Journal of Geophysical Research*, *114*, B09203. https://doi.org/10.1029/2008JB006228
Vandemeulebrouck, J., Sohn, R. A., Rudolph, M. L., Hurwitz, S., Manga, M., Johnston, M. J. S., et al. (2014). Eruptions at Lone Star geyser, Yellowstone National Park, USA: 2. Constraints on subsurface dynamics. *Journal of Geophysical Research: Solid Earth*, *119*, 8688–8707. https://doi.org/10.1002/2014JB011526
Vargas, C. A., Koulakov, I., Jaupart, C., Gladkov, V., Gomez, E., El Khrepy, S., & Al-Arifi, N. (2017). Breathing of the Nevado del Ruiz volcano reservoir, Colombia, inferred from repeated seismic tomography. *Scientific Reports*, *7*, 46,094.
Wallace, P. J. (2005). Volatiles in subduction zone magmas: Concentrations and fluxes based on melt inclusion and volcanic gas data. *Journal of Volcanology and Geothermal Research*, *140*(1), 217–240.
White, R., & McCausland, W. (2016). Volcano-tectonic earthquakes: A new tool for estimating intrusive volumes and forecasting eruptions. *Journal of Volcanology and Geothermal Research*, *309*, 139–155.
Wicks, C., de La Llera, J. C., Lara, L. E., & Lowenstern, J. (2011). The role of dyking and fault control in the rapid onset of eruption at Chaitén volcano, Chile. *Nature*, *478*(7369), 374–377. https://doi.org/10.1038/nature10541

References From the Supporting Information

Argus, D. F., Gordon, R. G., & DeMets, C. (2011). Geologically current motion of 56 plates relative to the no-net-rotation reference frame. *Geochemistry, Geophysics, Geosystems*, *12*, Q11001. https://doi.org/10.1029/2011GC003751
Calvert, A. T., Fierstein, J., & Hildreth, W. (2018). Eruptive history of Middle Sister, Oregon Cascades, USA—Product of a late Pleistocene eruptive episode. *Geosphere*, *14*(5), 2118–2139.
Carn, S. A., Fioletov, V. E., McLinden, C. A., Li, C., & Krotkov, N. A. (2017). A decade of global volcanic SO_2 emissions measured from space. *Scientific Reports*, *7*, 44,095.
Comeau, M. J., Unsworth, M. J., Ticona, F., & Sunagua, M. (2015). Magnetotelluric images of magma distribution beneath Volcán Uturuncu, Bolivia: Implications for magma dynamics. *Geology*, *43*(3), 243–246.
Flusser, J., Suk, T., & Zitová, B. (2016). *2D and 3D image analysis by moments*. Hoboken, NJ: John Wiley & Sons.

Fournier, R. O. (1999). Hydrothermal processes related to movement of fluid from plastic into brittle rock in the magmatic-epithermal environment. *Economic Geology*, *94*(8), 1193–1211. https://doi.org/10.2113/gsecongeo.94.8.1193

Heuret, A., & Lallemand, S. (2005). Plate motions, slab dynamics and back-arc deformation. *Physics of the Earth and Planetary Interiors*, *149*(1–2), 31–51.

Hildreth, W. (2007). Quaternary magmatism in the cascades: Geologic perspectives (pp. 1–125). US Geological Survey.

Hill, G. J., Bibby, H. M., Ogawa, Y., Wallin, E. L., Bennie, S. L., Caldwell, T. G., et al. (2015). Structure of the Tongariro volcanic system: Insights from magnetotelluric imaging. *Earth and Planetary Science Letters*, *432*, 115–125. https://doi.org/10.1016/j.epsl.2015.10.003

Jaxybulatov, K., Koulakov, I., Ibs-von Seht, M., Klinge, K., Reichert, C., Dahren, B., & Troll, V. R. (2011). Evidence for high fluid/melt content beneath Krakatau volcano (Indonesia) from local earthquake tomography. *Journal of Volcanology and Geothermal Research*, *206*(3), 96–105.

McTigue, D. F. (1987). Elastic stress and deformation near a finite spherical magma body: Resolution of the point source paradox. *Journal of Geophysical Research*, *92*, 12,931–12,940.

Mogi, K. (1958). Relations between the eruptions of various volcanoes and the deformations of the ground surfaces around them. *Bulletin of the Earthquake Research Institute*, *36*, 99–134.

Tamura, J., & Okada, T. (2016). Ambient noise tomography in the Naruko/Onikobe volcanic area, NE Japan: Implications for geofluids and seismic activity. *Earth, Planets and Space*, *68*(1), 1.